Resonant tunnelling at far infra-red frequencies

1994 J. Phys.: Condens. Matter 6 3945

(http://iopscience.iop.org/0953-8984/6/21/019)

J. Phys.: Condens. Matter 6 (1994) 3945–3954. Printed in the UK

Resonant tunnelling at far infra-red frequencies

V A Chitta†‖, C Kutter†, R E M de Bekker†, J C Maan†¶, S J Hawksworth‡, J M Chamberlain‡, M Henini‡ and G Hill§

† Max-Planck-Institut für Festkörperforschung, HML, BP 166, F-38042, Grenoble Cédex 9, France

‡ Department of Physics, Nottingham University, Nottingham NG7 2RD, UK

§ Department of Electronic and Electrical Engineering, University of Sheffield, Sheffield S1 3JD, UK

Received 21 December 1993

Abstract. The influence of far infra-red (FIR) radiation on the tunnel current of GaAs/GaAlAs double-barrier resonant tunnelling structures is investigated both experimentally and theoretically. For a tunnelling process characterized by a transmission coefficient with a full width at half maximum Γ_c, which is smaller than the photon energy $\hbar\omega$, a theoretical FIR response which depends on the radiation energy is obtained while, for a tunnelling process with Γ_c larger than $\hbar\omega$, this energy dependence is not observed. Although a clear dependence on the radiation energy could not be observed experimentally we show that a classical rectification cannot explain the obtained FIR response.

1. Introduction

Resonant tunnelling of electrons through semiconductor double-barrier heterostructures has attracted a great deal of attention both experimentally and theoretically because of its fundamental and technological importance. Following the pioneering work of Esaki and Tsu [1], many detailed studies aimed at understanding the basic physical processes of resonant tunnelling have been reported [2–5]. In particular, the shape of the bias dependence of the tunnelling current under both DC and AC voltages has been largely investigated [6–14]. Despite these studies, several fundamental aspects remain not understood. For example, the frequency limit of the AC response [15–19] and the tunnelling time [20–24] have not yet been determined satisfactorily. Even more elementary, we cannot unambiguously determine, from a simple analysis of the shape of the measured current–voltage $I(V)$ curves, whether tunnelling is coherent or sequential [15, 25–31] .

One of the most important characteristics of double-barrier heterostructures is their extremely fast electrical response which has been shown in their application as detectors up to 2.5 THz [32] and quantum well oscillators up to 420 GHz [33]. Following these experiments we investigate in this paper both theoretically and experimentally the influence of far infra-red (FIR) radiation on the tunnel current of double barrier resonant tunnelling structures (DBRTSs). We have been able to extend the detection limit up to 3.3 THz and more

‖ Present address: Instituto de Física e Química de São Carlos, Universidade de São Paulo, Caixa Postal 369, 13560-970 São Carlos, SP, Brazil.

¶ Present address: High Field Magnet Laboratory, Research Institute for Materials, University of Nijmegen, 6525 ED, Nijmegen, The Netherlands.

0953-8984/94/213945+10$19.50

importantly we show that in this limit classical rectification cannot explain the obtained FIR response [34,35], as was the case for Sollner *et al* [32].

This paper is organized as follows. A theoretical study of the FIR response of a DBRTS using the transfer matrix formalism is given in section 2. Considering tunnelling to be coherent, i.e. the phase of the wavefunction remains conserved on a time scale long with respect to the inverse radiation frequency, it is found that the calculated transmission coefficient exhibits characteristic satellite peaks at energies $\pm n\hbar\omega$ around the DC transmission peak, due to the absorption and emission of n photons. Obviously this behaviour gives rise to an FIR response which depends on the radiation energy characterizing a quantum response. In the case where the inverse of the radiation frequency is larger than the characteristic tunnelling time the satellite peaks are masked by the main peak in the transmission coefficient. Hence, the FIR response reduces to the classical result in which it is proportional to the second derivative of the $I(V)$ curve and independent of the radiation energy, characterizing a classical rectification.

The measured FIR response for three different devices, studied in the regime where a quantum detection is expected, is discussed in section 3. A clear deviation from the classical rectification regime can be observed, but the measured FIR response does not show a dependence on the FIR radiation energy as expected. Since we can exclude a trivial temperature effect on the basis of further experimental facts, these results show that in our samples the characteristic tunnelling time is longer that we expect theoretically.

2. Theory

The effect of FIR radiation (periodic modulation in time with frequency ω) superimposed on the DC voltage applied to a DBRTS can be described using a time-dependent extension [8] of the transfer matrix formalism [6], in which a time-dependent potential $U_1(z,t) = U_1(z)\cos(\omega t)$ is superimposed on the DC potential $U_0(z)$ (with $U_0(z)$ and $U_1(z)$ linear in z).

To obtain the current density $J(V)$ for this device we must calculate the transmission coefficient by solving the time-dependent Schrödinger equation:

$$i\hbar\frac{\partial\psi}{\partial t} = \left[-\frac{\hbar^2}{2m^*}\frac{\partial^2}{\partial z^2} + U_0(z) + U_1(z)\cos(\omega t)\right]\psi. \tag{1}$$

The tunnelling probability is obtained using the potential described above approximated by a series of steps, in which $U_0(z)$ and $U_1(z)$ are taken as constants. As demonstrated by Mendez [36], this approximation gives a result almost indistinguishable from an exact solution even for a small number of steps. For each region of constant potential, a general solution of equation (1) can be given as

$$\psi(z,t) = \int_{-\infty}^{+\infty}\left(A_\varepsilon e^{ikz} + B_\varepsilon e^{-ikz}\right)\exp\left(-\frac{i\varepsilon t}{\hbar}\right)\sum_{n=-\infty}^{\infty}J_n(\alpha)e^{-in\omega t}d\varepsilon \tag{2}$$

where k is given by

$$k(E) = \sqrt{\frac{2m^*[E - U_0(z)]}{\hbar^2}} \tag{3}$$

and $J_n(\alpha)$ is the integer Bessel function with $\alpha = U_1/\hbar\omega$. $A_{E'}$ and $B_{E'}$ are the amplitudes of the electron wavefunction with energy $E' = E \pm n\hbar\omega$. In the presence of a radiation an infinite number of these amplitudes are, in principle, necessary to describe the transmission and the reflection in the structure. However, the values of $A_{E'}$ and $B_{E'}$ depend on the radiation intensity (U_1) and for a fixed U_1 they decrease very fast as n increases. Hence, for a small value of U_1, only a finite small number of amplitudes determine the transmission coefficient reliably. By matching wavefunctions (2) at boundaries, and applying the transfer matrix formalism described in [8], the transmission coefficient, for a given number of amplitudes, can be calculated.

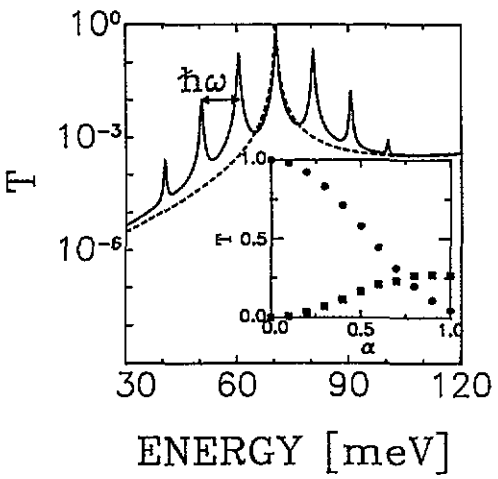

Figure 1. Calculated transmission coefficient of a DBRTS with a 5 nm thick GaAs quantum well and 5 nm thick $Ga_{0.7}Al_{0.3}As$ barriers in the absence of radiation (dashed line) and with applied radiation (solid line) characterized by a photon energy $\hbar\omega = 10$ meV and $\alpha = U_1/\hbar\omega = 0.5$. Satellite peaks up to the order $n = 3$ are shown. The inset shows the amplitude of the main transmission peak $E = E_0$ (closed circles) and the amplitude of the satellite at energy $E = E_0 - \hbar\omega$ (closed squares) as a function of the AC electric field of the applied radiation $\alpha = U_1/\hbar\omega$ with photon energy $\hbar\omega = 10$ meV.

The transmission coefficient at zero DC bias voltage for a DBRTS with 5 nm thick GaAs quantum well and 5 nm thick $Ga_{0.7}Al_{0.3}As$ barriers is shown in figure 1 for $\hbar\omega = 10$ meV, $\alpha = 0.5$ and $n = 3$. In the absence of applied radiation the transmission coefficient is given by the dashed line, and as is well known, a transmission peak is obtained when the energy of the incident electron coincides with the energy of the quasi-bound state inside the quantum well ($E_0 = 70.5$ meV). Since the structure is symmetric, the maximum of the transmission peak is equal to one, and it has a full width at half maximum of $\Gamma_c = 0.5$ meV, which is determined by the quantum well width and the barriers' height and thicknesses. The transmission coefficient obtained in the presence of FIR radiation ($\hbar\omega > \Gamma_c$) is given by the solid line, and shows a small decrease of the main peak at $E = E_0$ and the appearance of satellite peaks at energies $E = E_0 \pm \hbar\omega$. The amplitude of these transmission peaks depends on α ($\alpha = U_1/\hbar\omega$) as shown in the inset of figure 1. For a fixed energy ($\hbar\omega = 10$ meV), an increase of the radiation intensity U_1, i.e. an increase of α, produces a rapid decrease of the main E_0 peak (closed circles) and a slow increase of the satellite peaks (closed squares—peak at energy $E = E_0 - \hbar\omega$, $n = 1$). Figure 1 demonstrates that the

amplitude of the transmission peaks indeed decreases very rapidly with increasing n for a fixed value of α, and that the calculation may be performed for a limited n, sufficient to ensure that, for the values of α which are in the range of our interest, this has no effect on the results. For a photon energy $\hbar\omega$ smaller than Γ_c, the transmission coefficients obtained in the presence and absence of radiation are identical, i.e. the satellite peaks are masked by the E_0 transmission peak.

The only experimentally accessible component of the current in the very-high-frequency case is the DC current density $J(V)$, which we calculate using the transmission coefficient, $T(E, V)$ obtained above:

$$J(V) = \frac{e}{4\pi^3\hbar}\int_0^\infty \mathrm{d}k_\perp \int_0^\infty \mathrm{d}k_\parallel \left[f(E) - f(E')\right] T(E, V)\frac{\partial E}{\partial k_\parallel}. \tag{4}$$

Here $k_\perp$ and $k_\parallel$ are the components of the momentum perpendicular and parallel to the layers, E and E' the energies of the incident and transmitted electrons respectively, while $f(E)$ is the Fermi–Dirac distribution.

The $J(V)$ curve, as a result of having a transmission coefficient which shows satellite peaks due to the radiation, changes in a characteristic manner. The onset and the valley current increase, while the peak current decreases. Without radiation these values are given by $V_o = 2(E_0 - E_F)$ (onset) and $V_v = 2E_0$ (valley), where E_F is the Fermi energy in the emitter. With radiation they become $V_o' = 2(E_0 - \hbar\omega - E_F)$ and $V_v' = 2(E_0 + \hbar\omega)$ shifting the threshold of the onset current to lower bias and the threshold of the valley current to higher bias. Since the number of electrons that participates to the tunnelling is the same in both cases, the peak current must decrease in the presence of radiation to compensate the increase in the onset and valley currents.

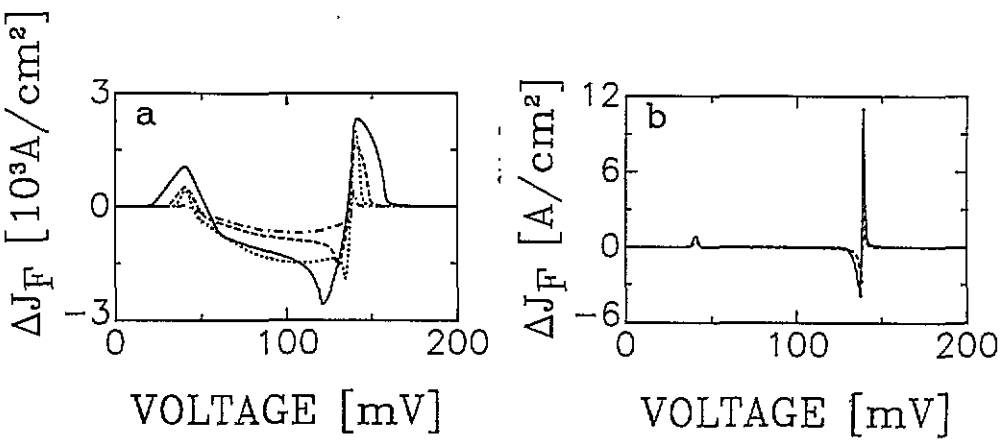

Figure 2. (a) Calculated FIR response for applied radiation with $\alpha = 0.5$ and different photon energies: $\hbar\omega = 10$ meV (solid line), $\hbar\omega = 5$ meV (dashed line), $\hbar\omega = 2.5$ meV (dotted line), and $\hbar\omega = 1$ meV (dashed-dotted line). (b) Comparison between the calculated FIR response for photon energy $\hbar\omega = 0.5$ meV and $\alpha = 0.1$ (solid line) and the second derivative of the $J(V)$ curve without radiation (dashed line).

In figure 2 we plot the changes in the current density due to the radiation, as a function of the DC bias voltage $\Delta J_F(V)$ (FIR response). Depending on the radiation energy with

respect to the full width at half maximum (Γ_c) of the transmission coefficient, $\Delta J_F(V)$ behaves in two different manners. For $\hbar\omega > \Gamma_c$, the FIR response depends clearly on $\hbar\omega$ (figure 2(a)) (quantum response), while for $\hbar\omega < \Gamma_c$ $\Delta J_F(V)$ is proportional to the second derivative of the $J(V)$ curve (figure 2(b)) (classical rectification). Since Γ_c is direct related to the steepness of the $J(V)$ curve, we can describe these two behaviours with the following condition [37]:

$$\left[J_{DC}\left(V + \frac{\hbar\omega}{e}\right) - J_{DC}(V)\right] \gg \left[J_{DC}(V) - J_{DC}\left(V - \frac{\hbar\omega}{e}\right)\right] \tag{5}$$

where J_{DC} is the current density without applied radiation, V is the DC bias voltage, and $\hbar\omega$ is the photon energy. This criterion is valid for small values of α ($U_1/\hbar\omega$). If it is satisfied, i.e. if the photon energy is high compared with the non-linearities of the $J(V)$ curve (or $\hbar\omega > \Gamma_c$), a clear dependence of $\Delta J_F(V)$ on the radiation energy can be expected (figure 2(a)). At low photon energies ($\hbar\omega < \Gamma_c$), the condition is no longer satisfied, and the shape of $\Delta J_F(V)$ as a function of the bias voltage is independent of $\hbar\omega$ and proportional to the second derivative of $J(V)$ (figure 2(b). In fact this response is just that of a single strongly non-linear impedance modulated by a small-amplitude time-varying voltage. The non-linearity gives rise to an AC response in the form of the second derivative, which is just classical rectification. In summary we can therefore conclude that when the condition given by (5) is satisfied, the changes in the tunnel current of a DBRTS due to the applied radiation will be due to quantum detection. Furthermore, the shape of $\Delta J_F(V)$ will show a dependence on the radiation energy. For low photon energies, for which (5) is not satisfied, the changes in the tunnel current are just those due to classical rectification, i.e. $\Delta J_F(V)$ will be proportional to the second derivative of $J(V)$. (5) was originally derived by Tucker [37] to describe the frequency-dependent response of devices which involve tunnelling through a single barrier (Schottky diodes, Josephson junction). According to our results his result can be extended to DBRTSs, which involve a double barrier and a non-linearity induced by a Fabry–Perot type interference.

3. Experiments

We have measured the FIR response of three DBRTSs, devices I, II, and III, grown by Molecular Beam Epitaxy (MBE) which consist of the following layers: (i) a GaAs substrate heavily doped with Si (electron concentration $n = 2 \times 10^{18}$ cm^{-3}); (ii) a 2 μm thick buffer layer of GaAs doped at $n = 2 \times 10^{18}$ cm^{-3}; (iii) 50 nm of doped GaAs ($n = 2 \times 10^{16}$ cm^{-3}); (iv) a 2.5 nm thick spacer layer of undoped GaAs; (v) an undoped 5.6 nm thick $Ga_{0.6}Al_{0.4}As$ barrier; (vi) an undoped GaAs quantum well; (vii) an undoped 5.6 nm thick $Ga_{0.6}Al_{0.4}As$ barrier; (viii) a 2.5 nm thick spacer layer of undoped GaAs; (ix) 50 nm of doped GaAs ($n = 2 \times 10^{16}$ cm^{-3}); and (x) a 0.5 μm top contact layer of GaAs ($n = 2 \times 10^{18}$ cm^{-3}). Devices I, II, and III are identical apart from the quantum well width (vi) which is equal to 5, 60, and 120 nm respectively. Squares mesas ranging from 200×200 μm^2 up to 500×500 μm^2 were etched and ohmic contacts made to the substrate and top layer.

The experiments have been performed at liquid He temperature using an FIR laser pumped by a pulsed TEA CO_2 laser (Lumonics 820). FIR pulses of 100 ns width and power higher than 10 W have been used with wavelength ranging from $\lambda = 90.9$ μm up to $\lambda = 496$ μm, which corresponds to photon energies ranging from $\hbar\omega = 13.6$ meV down to $\hbar\omega = 2.5$ meV respectively.

In order to couple the radiation to the confined electrons inside the quantum well it is necessary to have a component of the AC electric field from the radiation perpendicular to the layers (parallel to the current) [38]. To obtain this, we have used the top ohmic contact with a grating coupler geometry [39] which is shown schematically in the inset of figure 4. The grating consists of periodic metallic (AuGeNi) strips (strip width p and periodicity a) evaporated and allowed to the top n^+ layer. To act as a coupler the grating must satisfy some conditions. The first condition is that its periodicity a must be much smaller than the wavelength of the radiation, $a \ll \lambda$. For a normally incident radiation (z direction), the component of the electric field in the plane of the layers (perpendicular to the strips—x direction) E_x, is short-circuited in the strips. At the same time, the E_y component (parallel to the strips) is reflected. Thus, in the near field of the grating ($z < a$), the FIR field is spatially modulated and a component of the FIR electric field perpendicular to the layers, E_z, is obtained (as well as an E_x component). The intensity of E_z depends on the ratio p/a and decreases approximately as $\exp(-2\pi z/a)$ [40,41]. Hence, we can summarize the conditions that the grating must satisfy as: $a \ll \lambda$, $a \gg d$, and $p \ll a$, where d is the distance between the grating and the active region of the sample. For our samples we have chosen $a = 50$ μm and $p = 10$ μm.

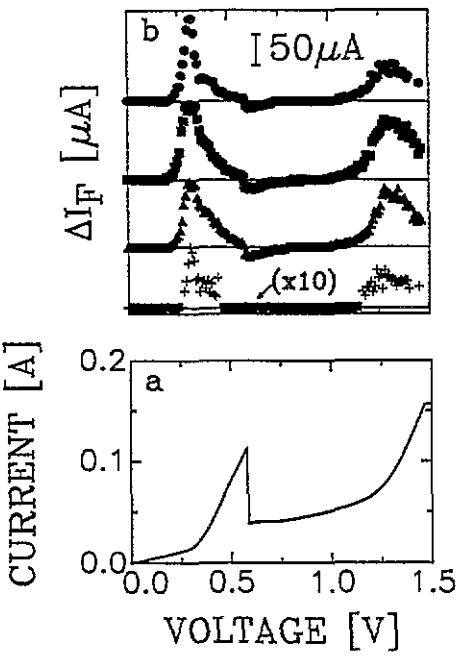

Figure 3. Current–voltage characteristic (a) and FIR response (b) measured for device I at 4.2 K. The applied FIR radiation is characterized by $\lambda = 90.9$ μm ($\hbar\omega = 13.6$ meV)—closed circles, $\lambda = 151$ μm ($\hbar\omega = 8.2$ meV)—closed squares, $\lambda = 292$ μm ($\hbar\omega = 4.2$ meV)—closed triangles, and $\lambda = 496$ μm ($\hbar\omega = 2.5$ meV)—crosses.

The measured FIR response $\Delta I_F(V)$ for device I—5 nm quantum well—is shown in figure 3 for four different FIR wavelengths together with its DC current–voltage $I(V)$ characteristic. In the present measurements, the negative differential resistance (NDR) region of the $I(V)$ curve of this sample is not clearly observed, possibly due to the contact resistance of the sample which leads to the sharp drop in the current at DC bias voltage $V \simeq 0.6$ V. For

all applied FIR radiation energies, $\Delta I_F(V)$ exhibits a similar behaviour. Positive maxima are observed at bias voltages which coincide with the onset of the NDR regions of the $I(V)$ curve. A negative minimum is also observed just after the sharp drop in the $I(V)$ curve, except for FIR energy $\hbar\omega = 2.5$ meV ($\lambda = 496$ μm) probably due to the small intensity of this line.

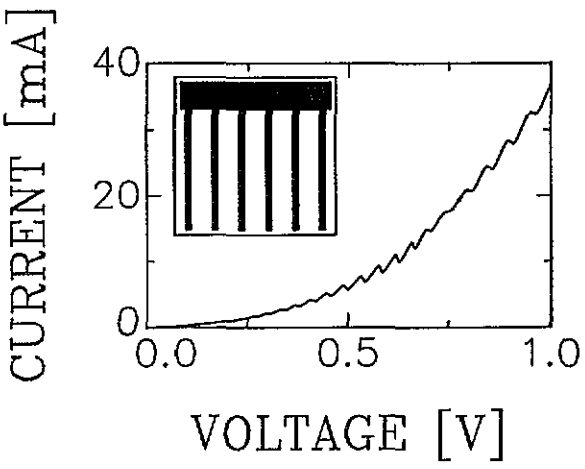

Figure 4. *Current–voltage characteristic of device* III *measured at 4.2 K. The inset shows* schematically the top ohmic contact of a mesa with the grating coupler geometry used.

Devices II and III have a qualitatively similar $I(V)$ characteristic and hence a similar behaviour of the FIR response. We show in figures 4 and 5 typical results of device III—120 nm quantum well. Due to the large number of resonant states inside this wide quantum well, its $I(V)$ characteristic consist of a series of closely spaced NDR regions (figure 4) [42]. Special attention has been focused on two adjacent NDR regions (figure 5(a)). Because of this small energy spacing the valley region of an NDR region coincides with the onset of the next NDR, giving an FIR response (figure 5(b)) which shows positive maxima in the valley regions and negative minima which almost coincide with the peaks of the $I(V)$ curve.

Applying the criterion given by equation (5) to analyse the FIR response of device I we can see that even for $\hbar\omega = 13.6$ meV, it is not satisfied for any voltage, except where the sharp drop of the current occurs in the valley region. However this sharp drop is not due to the DBRTS itself, but it is probably caused by the resistance of the contacts. Since, as we said above, the steepness of the $I(V)$ curve is directly related to the full width at half maximum Γ_c of the transmission coefficient, the actual Γ_c of device I should be larger than $\hbar\omega = 13.6$ meV. Comparing this Γ_c with the one calculated from the parameters of the device (well width and barrier height and thickness) $\Gamma_c = 0.5$ meV, we notice a broadening of the transmission coefficient. This broadening can be caused by a series of factors, among them we can have scattering by impurities, layer thickness fluctuations, phonons, etc. Experimentally, this broadening of the transmission coefficient yields an FIR response which is proportional to the second derivative of the $I(V)$ characteristic for all the photon energies used. Interestingly enough this experiment shows that classical rectification in DBRTS may be observed at frequencies as high as 3.3 THz.

For devices II and III the $I(V)$ characteristic is highly non-linear and equation (5) is satisfied (in the valley regions of the $I(V)$ curves) even for energies lower than 13.6

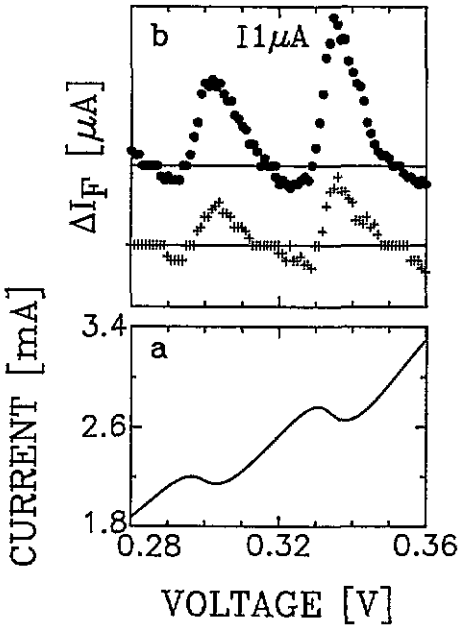

Figure 5. (a) Two consecutive negative differential resistance regions of the I(V) curve of device III for which the measured FIR response is shown in (b) for applied FIR radiation with wavelength $\lambda = 90.9\mu m$ ($\hbar\omega = 13.6$ meV)—closed circles and $\lambda = 496$ μm ($\hbar\omega = 2.5$ meV)—crosses.

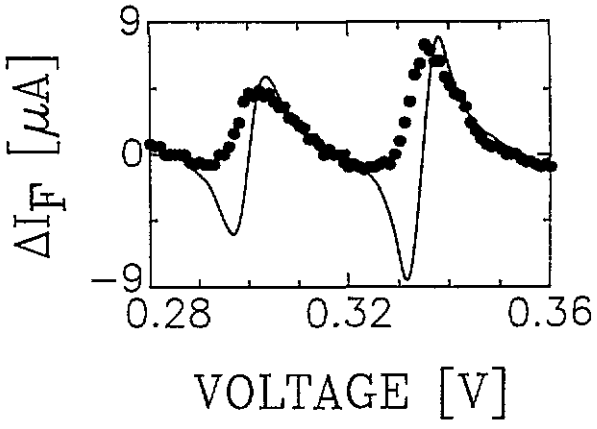

Figure 6. Comparison between the measured FIR response of device III (closed circles) for photon energy $\hbar\omega = 13.6$ meV and the second derivative of its $I(V)$ curve (solid curve).

meV. Therefore, on the basis of section II, a dependence on the radiation energy of the FIR response could be expected. However, the measured $\Delta I_F(V)$ (figure 5(b)) does not show a clear dependence on $\hbar\omega$. On the other hand, a comparison of the shape of the FIR response with that of d^2I/dV^2 (figure 6) shows that these are only similar in the regions where $I(V)$ is almost linear, but that a clear difference between the two exists in the highly non-linear regions. This observation may be interpreted as a sign that the threshold of the quantum detection regime is reached. A possible reason for the absence of a clear energy

dependence of the FIR response, although the condition of equation (5) is satisfied, could be the proximity of consecutive NDR regions of the $I(V)$ characteristic, which causes a superposition of the response of these NDR regions.

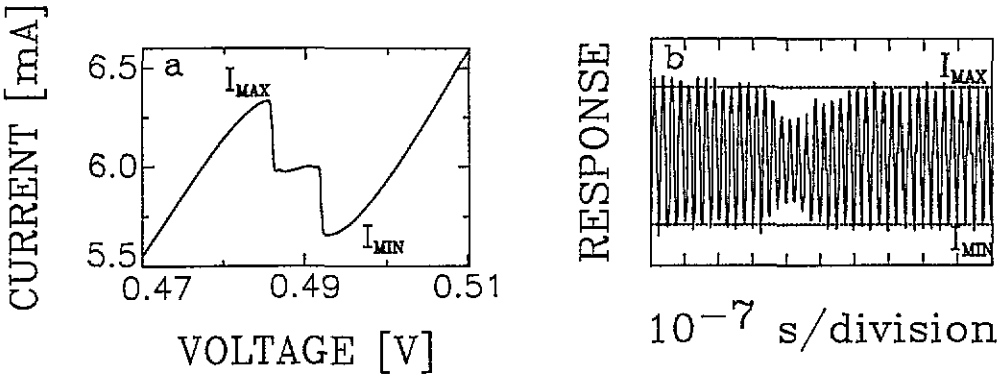

Figure 7. (a) Negative differential resistance region of the $I(V)$ characteristic of device III showing instability, where high frequency current oscillation can be observed as shown in (b). The amplitude of the oscillation ($\Delta I = I_{max} - I_{min}$) decreases when an FIR pulse is applied, leading to a rectification of the $I(V)$ curve.

For completeness we discuss the eventual possibility of lattice heating and/or carrier heating as an explanation of our results. In figure 7(a), one of the NDR regions of the $I(V)$ curve of device III is shown, in which instabilities can be observed (jumps and a plateau in between I_{max} and I_{min}). When the device is biased in the plateau, a high frequency oscillating current (with amplitude $\Delta I = I_{max} - I_{min}$) can be observed. If an FIR pulse is applied, the amplitude of the oscillations is squeezed (figure 7(b)), showing that the $I(V)$ curve is rectified. We can also see from figure 7(b) that the time resolution of the FIR response is of about 10 ns which is much shorter than the typical lattice heating of GaAs (of the order of μs), hence excluding this effect. Electronic heating can also be excluded since a similar $\Delta I_F(V)$ is obtained in forward and reverse bias operation, i.e. it is independent of whether the top contact through which the FIR radiation passes first is the emitter or the collector. Finally, we measured the change in the tunnel current due to an increase of the temperature and this curve is quite different from that of the FIR response. In particular, an increase of the temperature will never produce a decrease of the tunnel current as observed in the FIR response.

4. Conclusions

We have investigated both theoretically and experimentally the influence of FIR radiation on the tunnel current of DBRTSs. Theoretically we obtain, in the limit of high photon energies ($\hbar\omega$ larger than Γ_c, the full width at half maximum of the transmission coefficient), an FIR response that exhibits a clear dependence on the radiation energy. On the other hand, in the limit of much smaller photon energies, the FIR response is proportional to the second derivative of the $I(V)$ curve as expected from classical rectification.

We have shown experimentally that, depending on the $I(V)$ characteristic of the device studied, the classical rectification regime can, surprisingly, be extended up to frequencies as high as 3.3 THz. At the same time, for a different device with a much higher non-linear $I(V)$ characteristic, despite the fact that the measured FIR response does not exhibits a clear dependence on the FIR radiation energy, we have been able to show that a limit of quantum detection has been reached.

References

[1] Esaki L and Tsu R 1970 *IBM J. Res. Dev.* **14** 61
[2] Chang L L, Esaki L and Tsu R 1974 *Appl. Phys. Lett.* **24** 593
[3] Goldman V J, Tsui D C and Cunningham J E 1987 *Phys. Rev. Lett.* **58** 1256
[4] Tsuchiya M, Matsusue T and Sakaki H 1987 *Phys. Rev. Lett.* **59** 2356
[5] Hayden R K, Maude D K, Eaves L, Valadares E C, Henini M, Sheard F W, Hughes O H, Portal J C and Cury L 1991 *Phys. Rev. Lett.* **66** 1749
[6] Tsu R and Esaki L 1973 *Appl. Phys. Lett.* **22** 562
[7] Sokolovski D and Sumetskij M Y 1985 *Teor. Mat. Fiz.* **64** 233 Engl. Transl. 1985 *Theor. Math. Phys.* **64** 802)
[8] Coon D D and Liu H C 1985 *J. Appl. Phys.* **58** 2230
[9] Coon D D and Liu H C 1985 *Solid State Commun.* **55** 339
[10] Ohnishi H, Inata T, Muto S, Yokoyama N and Shibatomi A 1986 *Appl. Phys. Lett.* **49** 1248
[11] Cahay M, McLennan M, Datta S and Lundstrom M S 1987 *Appl. Phys. Lett.* **50** 612
[12] Frensley W R 1987 *Phys. Rev.* B **36** 1570
[13] Johansson P 1990 *Phys. Rev.* B **41** 9892
[14] Cai W, Zheng T F, Hu P, Lax M, Shum K and Alfano R R 1990 *Phys. Rev. Lett.* **65** 104
[15] Pan D S and Meng C C 1987 *J. Appl. Phys.* **61** 2082
[16] Sollner T C L G, Brown E R, Goodhue W D and Le H Q 1987 *Appl. Phys. Lett.* **50** 332
[17] Luryi S 1985 *Appl. Phys. Lett.* **47** 490
[18] Jogai B, Wang K L and Brown K D 1986 *Appl. Phys. Lett.* **48** 1003
[19] Coon D D and Liu H C 1986 *Appl. Phys. Lett.* **49** 94
[20] Büttiker M and Landauer R 1982 *Phys. Rev. Lett.* **49** 1739
[21] Collins S, Lowe D and Barker J R 1987 *J. Phys. C: Solid State Phys.* **20** 6213
[22] Hauge E H, Falck J P and Fieldly T A 1987 *Phys. Rev.* B **36** 4203
[23] Jauho A P and Jonson M 1989 *J. Phys.: Condens. Matter* **1** 9027
[24] Leavens C R and Aers G C 1989 *Phys. Rev.* B **39** 1202
[25] Stone A D and Lee P A 1985 *Phys. Rev. Lett.* **54** 1196
[26] Payne M C 1986 *J. Phys. C: Solid State Phys.* **19** 1145
[27] Weil T and Vinter B 1987 *Appl. Phys. Lett.* **50** 1281
[28] Jonson M and Grincwajg A 1987 *Appl. Phys. Lett.* **51** 1729
[29] Bütikker M 1988 *IBM J. Res. Dev.* **32** 63
[30] Gupta R and Ridley B K 1988 *J. Appl. Phys.* **64** 3089
[31] Jauho A P 1990 *Phys. Rev.* B **41** 12 327
[32] Sollner T C L G, Goodhue W D, Tannenwald P E, Parker C D and Peck D D 1983 *Appl. Phys. Lett.* **43** 588
[33] Brown E R, Sollner T C L G, Parker C D, Goodhue W D and Cheng C L 1989 *Appl. Phys. Lett.* **55** 1777
[34] Chitta V A, de Bekker R E M, Maan J C, Hawksworth S J, Chamberlain J M, Henini M and Hill G 1992 *Surf. Sci.* **263** 227
[35] Chitta V A, de Bekker R E M, Maan J C, Hawksworth S J, Chamberlain J M, Henini M and Hill G 1992 *Semicond. Sci. Technol.* **7** 432
[36] Mendez E E 1987 *Physics and Applications of Quantum Wells and Superlattices (NATO Advanced Study Institute Series B Physics)* ed E E Mendez and K von Klitzing (New York: Plenum)
[37] Tucker J C 1979 *IEEE J. Quantum Electron.* **QE-15** 1234
[38] Stern F 1974 *Phys. Rev. Lett.* **33** 960
[39] Tsui D C, Allen S J Jr, Logan R A, Kamgar A and Coppersmith S N 1976 *Surf. Sci.* **58** 104
[40] Allen S J Jr, Tsui D C and Logan R A 1977 *Phys. Rev. Lett.* **38** 980
[41] Zheng L, Schaich W L and MacDonald A H 1990 *Phys. Rev.* B **41** 8493
[42] Leadbeater M L, Alves E S, Eaves L, Henini M, Hughes O H, Celeste A, Portal J C, Hill G and Pates M A 1989 *J. Phys.: Condens. Matter* **1** 4865